

## Solid-state Carbon-13 Nuclear Magnetic Resonance Spectra of Selected Metal Carboxylate Complexes

Paul A. Hunt and Brian P. Straughan\*

*Department of Chemistry, The University, Newcastle upon Tyne NE1 7RU*

Ahmed A.M. Ali, Robin K. Harris, and Barry J. Say

*Department of Chemistry, University of Durham, South Road, Durham DH1 3LE*

Eight anhydrous metal carboxylate complexes have been studied in the solid state by  $^{13}\text{C}$  cross-polarization magic-angle-spinning n.m.r. spectroscopy. A general assignment of the  $^{13}\text{C}$  n.m.r. spectra can be made by comparing the data obtained with definitive structural data previously reported in single-crystal X-ray crystallographic studies. Although a complete assignment of all n.m.r. peaks has not been achieved, the results highlight the important parameters involved and demonstrate that in many cases definitive structural data can be deduced for these complexes in the solid state using n.m.r. spectroscopy. Metal carboxylates are excellent compounds for a comparative study because of the very high quality of the solid-state spectra produced. A crystallographic splitting of 8 Hz can be seen clearly in some spectra. The chemical shift is very sensitive to the precise crystallographic environment.

During the past five years we have prepared and structurally characterised a wide range of anhydrous metal carboxylate complexes by X-ray crystallography. This paper considers five of these complexes: zinc acetate,<sup>1</sup> propanoate,<sup>2</sup> crotonate,<sup>3</sup> 3,3-dimethylacrylate,<sup>4</sup> and lead crotonate<sup>5</sup> together with two basic zinc carboxylates {the hydroxy-centred crotonate<sup>6</sup> [ $\text{Zn}_5(\text{OH})_2(\text{MeCH}=\text{CHCO}_2)_8$ ] and the oxo-centred pivalate<sup>6</sup> [ $\text{Zn}_4\text{O}(\text{Me}_3\text{CCO}_2)_6$ ]}. Finally sodium crotonate has been included for comparative purposes even though its crystal structure has not been determined. In all cases the crotonate ligand has the *trans* structure.

High-resolution  $^{13}\text{C}$  solid-state n.m.r. spectra of these eight complexes have been studied to demonstrate that definitive structural conclusions can be obtained and to show that  $^{13}\text{C}$  n.m.r. spectroscopy is an important complementary technique to X-ray crystallography, as has been demonstrated for simple metal acetates.<sup>7</sup> In addition, it is a useful technique for the detection and identification of trace impurities which are not evident in a crystallographic determination.

### Experimental

The preparations of all of the complexes used are described in detail elsewhere.<sup>1-6</sup> The samples varied in their degree of crystallinity. Thus zinc propanoate, crotonate (see later for discussion), and 3,3-dimethylacrylate were highly crystalline, whereas sodium crotonate, zinc acetate, and basic zinc crotonate, [ $\text{Zn}_5(\text{OH})_2(\text{MeCH}=\text{CHCO}_2)_8$ ], normally precipitated out as powders.

These complexes were all washed with diethyl ether, dried over  $\text{P}_2\text{O}_5$  *in vacuo*, and were analysed by microanalysis (see Table 1) and i.r. spectroscopy. The analytical data are in good agreement with previously published data.

**Solid-state N.M.R. Spectroscopy.**—High-resolution  $^{13}\text{C}$  n.m.r. spectra of the solids were obtained using high-power proton decoupling, cross-polarization, and magic-angle spinning. A Bruker CXP 200 spectrometer was used, operating at 50.32 MHz and ambient probe temperature (*ca.* 30 °C). The samples were packed as crystalline powders (*ca.* 300 mg) into standard double-bearing rotors. Typical conditions were: contact time 5 ms; recycle delay 10 s; number of transients 500; acquisition



Figure 1. Diagram showing the *syn-anti* (left) and *syn-syn* (right) carboxylate bridging modes

4K points, zero-filled to 16K before Fourier transformation. Chemical shifts are reported on the high-frequency-positive scale with respect to the signal of tetramethylsilane *via* a replacement sample of adamantane (high-frequency line at  $\delta_{\text{C}} = 38.5$  p.p.m.). They are accurate to  $\pm 0.5$  p.p.m. absolutely (or to  $\pm 0.1$  p.p.m. internally for a given sample).

### Results and Discussion

The spectra obtained from the eight samples will be discussed individually. The chemical shift data are summarised in Table 2. It is of interest that the samples all gave excellent quality spectra; this could be attributed to various factors such as the highly ordered structures exhibited by the complexes. The n.m.r. spectra provide immediate information about the nature of the asymmetric crystallographic unit.

**Zinc Acetate.**—The sample used in this study is anhydrous zinc(II) acetate. It belongs to the monoclinic crystal system and the X-ray structure is given in ref. 1. It is in fact a three-dimensional polymer with the acetate ligands acting as *syn-anti* bridges (see Figure 1)<sup>8</sup> around the tetrahedrally co-ordinated zinc atoms.

The solid-state  $^{13}\text{C}$  n.m.r. spectrum indicates that there are two non-equivalent acetate groups, since the signals for both the methyl carbons (near 20 p.p.m.) and the carboxyl carbons (near 180 p.p.m.) show 1:1 splittings. This is consistent with the crystal structure of zinc acetate<sup>1</sup> which shows that there are two crystallographically inequivalent methyl and carboxylate groups present in the unit cell. The n.m.r. signal due to the carboxyl carbons has a splitting of 1.0 p.p.m., whilst the signal of

**Table 1.** Microanalytical data \* and morphology of samples

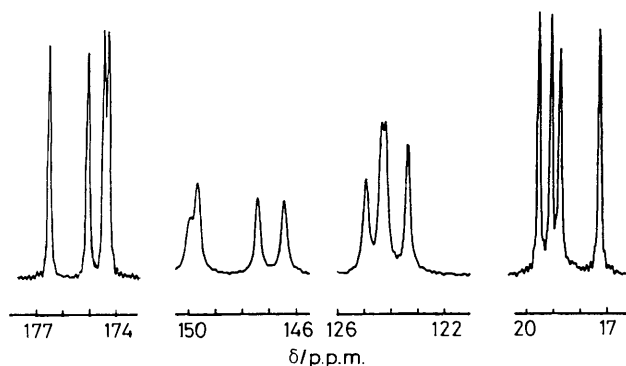
Compound	Analysis (%)				Morphology
	C		H		
	Calcd	Found	Calcd	Found	
Zn(MeCO <sub>2</sub> ) <sub>2</sub>	26.1	(26.2)	3.1	(3.3)	Powder
Zn(EtCO <sub>2</sub> ) <sub>2</sub>	34.0	(34.1)	4.6	(4.8)	Crystalline
Zn(MeCH=CHCO <sub>2</sub> ) <sub>2</sub>	40.6	(40.8)	4.1	(4.3)	Crystalline
Zn(Me <sub>2</sub> C=CHCO <sub>2</sub> ) <sub>2</sub>	45.5	(45.6)	5.3	(5.3)	Crystalline
Pb(MeCH=CHCO <sub>2</sub> ) <sub>2</sub>	25.4	(25.5)	2.6	(2.7)	Microcrystalline
[Zn <sub>5</sub> (OH) <sub>2</sub> (MeCH=CHCO <sub>2</sub> ) <sub>8</sub> ]	36.8	(36.9)	3.8	(4.1)	Powder
[Zn <sub>4</sub> O(Me <sub>3</sub> CCO <sub>2</sub> ) <sub>6</sub> ]	41.2	(40.7)	6.2	(6.1)	Powder
Na(MeCH=CHCO <sub>2</sub> )	44.4	(44.5)	4.6	(4.7)	Powder

\* Required values are given in parentheses.

**Table 2.** Carbon-13 n.m.r. chemical shift data (p.p.m. relative to SiMe<sub>4</sub>)

	Alkyl			Alkenyl			Carboxyl CO <sub>2</sub>
	CH <sub>3</sub>	CH <sub>2</sub>	C	3-CH	2-CH	3-C	
Zn(MeCO <sub>2</sub> ) <sub>2</sub>	21.6 23.3						183.2 184.2
Zn(EtCO <sub>2</sub> ) <sub>2</sub>	9.8 10.2	28.9 29.7					185.9
Zn(MeCH=CHCO <sub>2</sub> ) <sub>2</sub>	17.3 18.8 19.1 19.6			146.5 147.5 149.7 150.0 <sup>a</sup>	123.4 124.2 124.4 125.0		174.3 174.5 175.1 176.6
Zn(Me <sub>2</sub> C=CHCO <sub>2</sub> ) <sub>2</sub>	19.8, 26.6 20.9, 27.0 21.1, 28.6 21.5, 29.0				119.1 119.7 120.1 122.1	154.6 156.5 158.0 158.6	174.3 174.9 175.1 177.1
Pb(MeCH=CHCO <sub>2</sub> ) <sub>2</sub>	18.9 19.9			141.5 147.6	128.4 134.4 <sup>b</sup>		176.1 176.9
[Zn <sub>5</sub> (OH) <sub>2</sub> (MeCH=CHCO <sub>2</sub> ) <sub>8</sub> ]	17.4 17.5 17.9 19.3		39.8	141.9 144.4 ? 148.1	123.8 126.6 127.5 ?		174.1 174.5 176.9 177.7
[Zn <sub>4</sub> O(Me <sub>3</sub> CCO <sub>2</sub> ) <sub>6</sub> ]	29.2						191.2
Na(MeCH=CHCO <sub>2</sub> )	18.0			135.4	132.5		175.0

<sup>a</sup> Broad. <sup>b</sup> With satellite peaks.

**Figure 2.** <sup>13</sup>C N.m.r. spectrum of anhydrous zinc crotonate

the methyl carbon atoms shows a splitting of 1.7 p.p.m., *i.e.* the carbons closest to the metal atoms show the smaller splittings.

The X-ray data show only small (possibly not significant) differences between the geometries of the non-equivalent carboxylate groups, the largest being in the OCO angle [120.9(3) and 121.7(2)<sup>o</sup>]. However, the Zn-O distances for the two carbonyl groups do show significant variations [1.952(2) and 1.949(2) Å for one carbonyl, and 1.960(2) and 1.965(2) Å for the other] which makes it somewhat surprising that the crystallographic splitting for the carboxyl carbon is less than that for the methyl carbon (though of course methyl carbons are at the molecular periphery and therefore may be strongly influenced by intermolecular packing effects).

**Zinc Propanoate.**—The structure of this anhydrous salt is given in ref. 2. It is orthorhombic, and again contains two propanoate groups in the asymmetric unit. It is best described as having a two-dimensional sheet structure. The solid-state <sup>13</sup>C n.m.r. spectrum is analogous to that of anhydrous zinc acetate. There are three types of carbon for each propanoate ligand, a

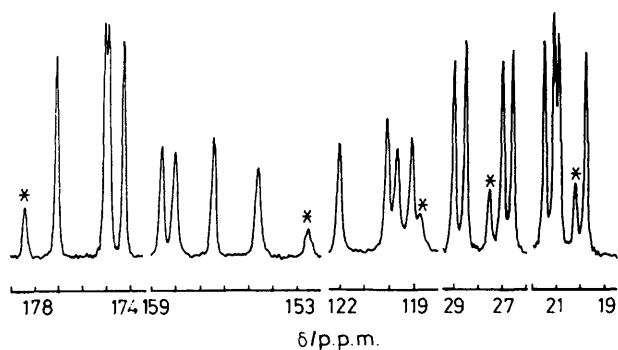


Figure 3.  $^{13}\text{C}$  N.m.r. spectrum of anhydrous zinc 3,3-dimethylacrylate. The asterisks indicate peaks assigned to an impurity (see text)

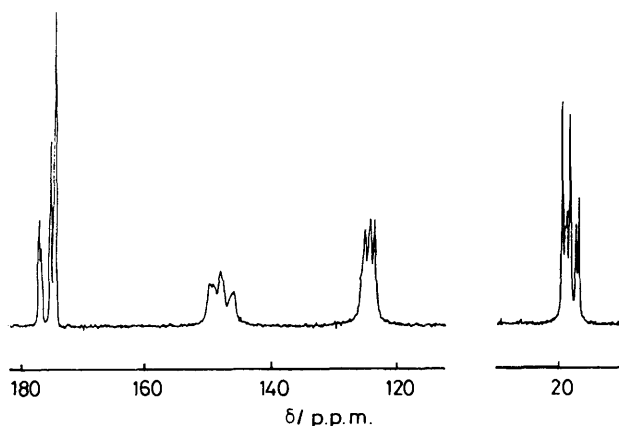


Figure 4.  $^{13}\text{C}$  N.m.r. spectrum of impure powdered zinc crotonate

methyl carbon (which exhibits two peaks at 9.8 and 10.2 p.p.m., *i.e.* a crystallographic splitting of 0.4 p.p.m.), a methylene carbon (with peaks at 28.9 and 29.7 p.p.m., and a crystallographic splitting of 0.8 p.p.m.), and a carboxyl carbon (which gives a single peak at 185.9 p.p.m., presumably because the crystallographic splitting is too small to resolve).

**Zinc Crotonate.**—The crystal structure shows this to be a one-dimensional polymeric chain,<sup>3,9</sup> in which there are four crotonate ligands present in the unit cell {three *syn-syn* bridges form a  $[\text{Zn}_2(\text{MeCH}=\text{CHCO}_2)_3]^+$  unit and a *syn-anti* bridge connects these units together}. Since each crotonate ligand has four different carbon atoms, a total of 16 lines is expected and observed (see Figure 2). The quality of the spectrum can be seen by the fact that peaks of splitting as low as 8 Hz can be clearly resolved. The methyl carbon signal occurs at around 18 p.p.m., the carboxyl carbon at around 175 p.p.m., while two olefinic carbon signals are observed at *ca.* 148 and 124 p.p.m. (for  $\text{Me}-\text{CH}=\text{}$  and  $=\text{CH}-\text{CO}_2$  respectively).

It is not possible to assign unambiguously peaks belonging to the *syn-anti* bridge and the  $[\text{Zn}_2(\text{MeCH}=\text{CHCO}_2)_3]^+$  cage; the peaks at 176.6 and 17.3 p.p.m. are separated from the other peaks in the group, but there is no definite proof that these are due to the *syn-anti* bridge as the separations are not excessive in comparison to other crystallographic splittings. One of the 3-CH peaks (at 150.0 p.p.m.) appears to be broader than the others, but the origin of this effect is not understood.

**Zinc 3,3-Dimethylacrylate.**—The crystal structure of this salt is analogous to that of zinc crotonate with four types of dimethylacrylate bridges present, three in the cage  $[\text{Zn}_2(\text{Me}_2\text{C}=\text{CHCO}_2)_3]^+$  with a single *syn-anti* bridging carboxylate

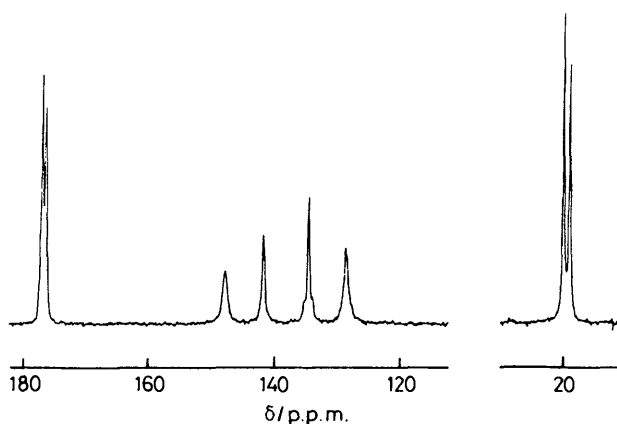


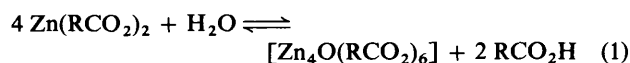
Figure 5.  $^{13}\text{C}$  N.m.r. spectrum of anhydrous lead crotonate

between the cages.<sup>5</sup> This time there are five carbon signals from each dimethylacrylate (see Figure 3) with the methyl signals occurring at around 20 and 27 p.p.m., the latter being *trans* to the carboxyl group. The carboxyl carbon itself shows a signal at around 175 p.p.m. while the olefinic carbons lie at 156 p.p.m. for the  $\text{Me}_2\text{C}=\text{}$  carbon and 120 p.p.m. for the  $\text{O}_2\text{CCH}=\text{}$  olefinic carbon. It is again the case that the  $\text{Me}_2\text{C}=\text{}$  olefinic carbon has its signal split to the largest extent with a maximum crystallographic splitting of 4 p.p.m. It might again be suggested that the peaks at 119.1, 154.6, 122.1, and 19.8 p.p.m. belong to the *syn-anti* bridge. However, there is no proof of this other than they appear at a position quite distinct from other peaks and that they fit into the pattern seen for zinc crotonate.

An interesting feature of the spectrum is the extra peak in each carbon region (indicated by asterisks in Figure 3). This suggests an impurity which we anticipate may be caused by the presence of some basic zinc 3,3-dimethylacrylate.

It is worth emphasizing the anhydrous nature of the zinc crotonate sample discussed above because an earlier powdered sample produced from the reaction of zinc hydroxide with crotonic acid gave a highly complex spectrum indicating the presence of far more than four types of crotonate environment. As this was clearly impossible from the crystal structure, further work was carried out to clear up this apparent inconsistency. Recrystallisation of the sample from reagent-grade ethanol gave anhydrous crystals, which resulted in the expected spectrum, discussed previously. It is interesting, however, that extra peaks which appear in the spectrum of the sample of powdered crotonate (Figure 4) are on the high-frequency side of the signals for the carboxyl carbons. This is also the case for the impurity in zinc 3,3-dimethylacrylate. The extra peak in the methyl carbon region appears towards the low-frequency side in both the powdered crotonate and 3,3-dimethylacrylate spectra. Two other peaks in the impure crotonate spectrum are not well resolved and do not allow a clear view of the impurity peaks, but there is a pattern emerging that suggests a similar type of impurity is present in both samples.

Recent studies in solution<sup>10</sup> have provided evidence for the presence of an equilibrium between normal and basic carboxylate species when the former is dissolved in wet organic solvents [equation (1)]. Zinc crotonate and 3,3-dimethylacrylate were



both prepared initially from aqueous solution<sup>9</sup> and were precipitated by the removal of water on a rotary evaporator. The products were washed with diethyl ether which would remove traces of free acid but would not remove small amounts

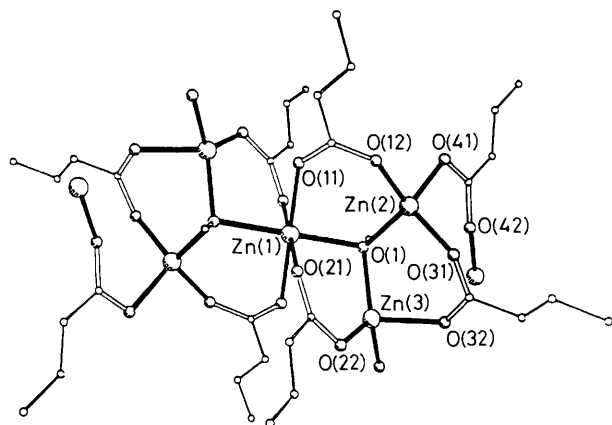


Figure 6. Molecular structure of basic zinc crotonate  $[\text{Zn}_5(\text{OH})_2(\text{MeCH}=\text{CHCO}_2)_8]$

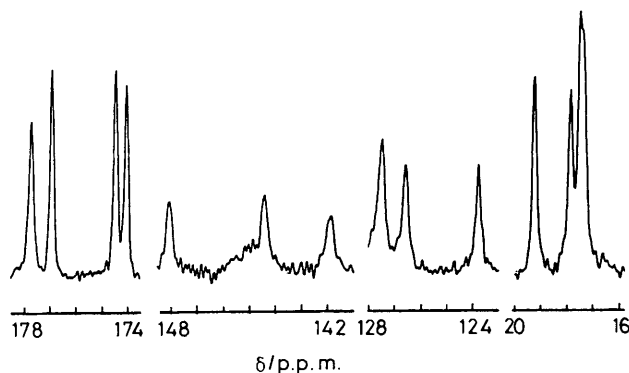


Figure 7.  $^{13}\text{C}$  N.m.r. spectrum of basic zinc crotonate

Table 3. Correlation between  $\text{p}K_a$  for acids used and  $\delta(\text{CO}_2)$  for the zinc salts

Acid	$\text{p}K_a^a$	$\delta(\text{CO}_2)/\text{p.p.m.}$ for zinc salt
$\text{Me}_3\text{CCO}_2\text{H}$	5.03	191.2
$\text{EtCO}_2\text{H}$	4.87	185.9
$\text{MeCO}_2\text{H}$	4.75	183.7 <sup>b</sup>
$\text{MeCH}=\text{CHCO}_2\text{H}$	4.44	175.1 <sup>b</sup>
$\text{Me}_2\text{C}=\text{CHCO}_2\text{H}$	5.12	175.4 <sup>b</sup>

<sup>a</sup> Taken from ref. 12. <sup>b</sup> Average value.

of the basic salt, present as an impurity in the normal anhydrous metal carboxylate. Purification can be achieved by recrystallisation of the impure carboxylate from reagent-grade ethanol. Thus we propose that the impurity peaks in the  $^{13}\text{C}$  n.m.r. spectra of both powdered zinc crotonate and zinc 3,3-dimethylacrylate are due to traces of the corresponding basic salt  $[\text{Zn}_4\text{O}(\text{RCO}_2)_6]$ .

**Lead Crotonate.**—The crystal structure of this salt<sup>4</sup> shows it to be a polymer containing two types of crotonate ligand; one is chelating to the lead alone and is not involved in the polymerisation while the other is part of the polymeric chain, chelating to one lead atom whilst forming monodentate bridges to the two adjacent lead atoms.

The spectrum (Figure 5) shows that there are two types of crotonate present in the structure, the signal of the methyl carbons being crystallographically split by 1.0 p.p.m., whilst the signal due to the carboxyl carbons is split by 0.8 p.p.m. The latter value is smaller than the crystallographic splitting of

the carboxyl carbon signals of zinc acetate (1 p.p.m.) in which this is caused by purely crystallographic inequivalence rather than chemical inequivalence as in this case. One would have expected that chemical inequivalence would cause a much greater crystallographic splitting and that this would allow easier structural elucidation; this is clearly not the case.

The remarkable aspect of the spectrum is the splitting of the two olefinic carbon signals. It could be suggested that they are paired *viz.* 147.6, 141.5 p.p.m. (for the  $\text{Me}-\text{CH}=\text{olefinic carbon}$ ) and 134.4, 128.4 p.p.m. (for the  $=\text{CH}-\text{CO}_2$  carbon). On this assumption they have crystallographic splittings of 6.1 and 6.0 p.p.m. respectively. There is no direct evidence as to why the double bonds seem so sensitive to metal environments whilst the other parts of the structures are less so. There are certainly no real differences in bond distances within the two groups so it is presumably a through-space phenomenon, the position of the peaks being determined by the closeness of surrounding chains in the lattice. Finally, it is apparent that there is broadening around the base of several of the olefinic carbon peaks. A possible cause of this might be some coupling to  $^{207}\text{Pb}$ , but such splittings are not visible for the carboxyl peaks. The  $^{207}\text{Pb}$  n.m.r. spectrum for this complex has been recorded in the solid state at 62.74 MHz using a Varian VXR 300 spectrometer. A very extensive set of spinning sidebands is seen, covering *ca.* 3 000 p.p.m. and indicating a large shielding anisotropy. The isotropic shift appears to be at  $\delta_{\text{pb}}$   $-727$  p.p.m. from the signal due to  $\text{PbMe}_4$ . Since the  $^{207}\text{Pb}$  n.m.r. spectrum shows a single centreband within the accuracy of the linewidth (*ca.* 400 Hz), the asymmetric unit must contain only one Pb atom (in agreement with the X-ray results).

**Basic Zinc Crotonate**  $[\text{Zn}_5(\text{OH})_2(\text{MeCH}=\text{CHCO}_2)_8]$ .—The asymmetric unit of this structure contains four crotonate bidentate bridges.<sup>6</sup> Its molecular structure in the crystalline state is shown in Figure 6. The n.m.r. spectrum (Figure 7) is consistent with this structure, but further discussion is necessary. It is clear that there are four peaks associated with both the methyl and the carboxyl carbons. However, the olefinic carbons do not clearly show four peaks; in the  $\text{Me}-\text{CH}=\text{olefinic carbon}$  signal there are three peaks plus a broad hump under the central peak at around 145 p.p.m. This broad hump is probably the 'missing' signal. The reason for the breadth of this signal is not known, but it parallels the case of zinc crotonate itself. In the  $=\text{CH}-\text{CH}_2$  olefinic carbon region there are three peaks, but one is more intense than the other two so perhaps two peaks overlap each other. Again in this spectrum the  $\text{Me}-\text{CH}=\text{olefinic carbon}$  shows the largest spread of signals (maximum crystallographic splitting of 6.2 p.p.m.).

**Basic Zinc Pivalate**  $[\text{Zn}_4\text{O}(\text{Me}_3\text{CCO}_2)_6]$ .—This structure is a well characterised  $\mu_4$ -oxo centred tetranuclear complex,<sup>6</sup> very similar to basic zinc acetate.<sup>11</sup> In the crystal structure an acetone molecule is found in the lattice. However, the sample examined by n.m.r. spectroscopy had lost this acetone due to breaking-up of the crystals by acetone diffusion out of the lattice.

The spectrum is extremely simple showing the existence of only one type of pivalate environment, which would point to a highly symmetrical  $[\text{Zn}_4\text{O}(\text{Me}_3\text{CCO}_2)_6]$  structure where all the pivalates are equivalent. When acetone is incorporated there is a small degree of asymmetry which produces inequivalency amongst the pivalate bidentate bridges, but the acetone is not present in the powdered n.m.r. sample. The three types of carbon present are easily identified; the quaternary carbons occur at 39.84 p.p.m., the methyl carbons are at 29.16 p.p.m., and the carboxyl carbons lie at 191.20 p.p.m.

A pattern is emerging for the particular position of a carboxyl carbon signal in a complex and the  $\text{p}K_a$  value of the acid used. For example pivalic acid has a high  $\text{p}K_a$  value and zinc pivalate

has the highest chemical shift for its carboxyl carbon peak. By studying the  $pK_a$  values for the acids used in this paper (Table 3) it is possible to identify a relationship with the chemical shift of the carboxyl carbon peak for the zinc complexes.

The pivalate has a highly electron-donating substituent on the carboxylate ligand which causes a deshielding effect on the carbonyl carbon. By contrast, the crotonate ligand has some conjugation between the double bond and the carbonyl group which withdraws electrons from the carboxylate group. It is not clear why the 3,3-dimethylacrylate salt does not fit into this general pattern.

*Sodium Crotonate.*—There is no crystal structure available for this complex, although *X*-ray powder diffraction work has recently been carried out.<sup>13</sup> The solid-state  $^{13}\text{C}$  n.m.r. spectrum shows that the complex has a simple structure with only one type of crotonate present; the methyl carbon occurs at 18.0 p.p.m. and the carboxyl carbon lies at 175.0 p.p.m. (very similar to the average position for zinc crotonate). The particularly interesting features of this spectrum are again the two peaks due to the olefinic carbons. For the complexes examined so far in this work a separation of at least 7 p.p.m. has been observed for these peaks. Indeed much larger separations of around 26 p.p.m. for zinc crotonate and 40 p.p.m. for zinc 3,3-dimethylacrylate have been observed. However for sodium crotonate the separation is only 2.9 p.p.m. An examination of all the crystallographic data for crotonate systems, including base adducts of zinc<sup>14,15</sup> and copper,<sup>9</sup> indicates that the dimensions within the crotonate group change very little among complexes; for example the C=C distances vary between 1.295 and 1.311 Å, which represents a range of only 1–2%. Thus the changes in signal positions cannot be explained simply in terms of a variation in bond distances.

In conclusion, it is clear from the present data that high-resolution  $^{13}\text{C}$  solid-state n.m.r. spectroscopy is an important complementary technique to *X*-ray crystallography. More information is potentially available for all of these systems from shielding-tensor anisotropies and asymmetries. In principle, these could be obtained from analysis of spinning sideband manifolds. It is feasible to derive such data for simple metal acetates and formates.<sup>16,17</sup> However, in the present spectra,

spinning speeds of *ca.* 4.5 kHz were employed and spinning sidebands are weak. Lower spinning rates would rapidly lead to confusing overlap of peaks, making the question of obtaining extra data difficult.

### Acknowledgements

One of us (A. A. M. A.) thanks the University of Kuwait for its generous provision of study leave. Thanks are also due to the S.E.R.C. for a maintenance grant (to P. A. H.).

### References

- 1 W. Clegg, I. R. Little, and B. P. Straughan, *Acta Crystallogr., Sect. C*, 1986, **42**, 1701.
- 2 W. Clegg, I. R. Little, and B. P. Straughan, *Acta Crystallogr., Sect. C*, 1987, **43**, 456.
- 3 W. Clegg, I. R. Little, and B. P. Straughan, *Acta Crystallogr., Sect. C*, 1986, **42**, 919.
- 4 W. Clegg, I. R. Little, and B. P. Straughan, unpublished work.
- 5 W. Clegg, I. R. Little, and B. P. Straughan, *Acta Crystallogr., Sect. C*, 1986, **42**, 1319.
- 6 W. Clegg, D. R. Harbron, I. R. Little, and B. P. Straughan, to be published.
- 7 C. J. Groombridge, R. K. Harris, K. J. Packer, M. B. Hursthouse, and N. P. C. Walker, *J. Solid State Chem.*, 1985, **59**, 306.
- 8 G. B. Deacon and R. J. Phillips, *Coord. Chem. Rev.*, 1980, **33**, 227.
- 9 I. R. Little, Ph.D. Thesis, University of Newcastle upon Tyne, 1986.
- 10 D. R. Harbron, P. A. Hunt, and B. P. Straughan, to be published.
- 11 H. Koyama and Y. Saito, *Bull. Chem. Soc. Jpn.*, 1954, **27**, 112.
- 12 G. Kortum, W. Vogel, and K. Andrussow, *Pure Appl. Chem.*, 1960, **1**, 190.
- 13 K. Naruchi and M. Miura, *J. Chem. Soc., Perkin Trans. 2*, 1987, 113.
- 14 W. Clegg, I. R. Little, and B. P. Straughan, *Inorg. Chem.*, 1988, **27**, 1916.
- 15 W. Clegg, I. R. Little, and B. P. Straughan, *J. Chem. Soc., Dalton Trans.*, 1986, 1283.
- 16 C. J. Groombridge, R. K. Harris, and K. J. Packer, *Bull. Magn. Reson.*, 1983, **5**, 189.
- 17 C. J. Groombridge, Ph.D. Thesis, University of East Anglia, 1983.

Received 17th August 1989; Paper 9/03534F